BIOCHEMISTRY
including biophysical chemistry & molecular biology

Article

pubs.acs.org/biochemistry

A Single Active-Site Mutation of P450BM-3 Dramatically Enhances Substrate Binding and Rate of Product Formation

Donovan C. Haines,*[,†] Amita Hegde,[‡] Baozhi Chen,[‡] Weiqiang Zhao,[§] Muralidhar Bondlela,[‡] John M. Humphreys,[‡] David A. Mullin,[⊥] Diana R. Tomchick,[‡] Mischa Machius,[‡] and Julian A. Peterson[‡]

[†]Department of Chemistry, Sam Houston State University, 1003 Bowers Blvd., Huntsville, Texas 77340, United States

[‡]Department of Biochemistry, The University of Texas Southwestern Medical Center at Dallas, 5323 Harry Hines Blvd., Dallas, Texas 75390-9038, United States

[§]The Ohio State University Medical Center, Columbus, Ohio 43210, United States

[⊥]Department of Cell and Molecular Biology, Tulane University, 2000 Percival Stern Hall, New Orleans, Louisiana 70118, United States

ABSTRACT: Identifying key structural features of cytochromes P450 is critical in understanding the catalytic mechanism of these important drug-metabolizing enzymes. Cytochrome P450BM-3 (BM-3), a structural and mechanistic P450 model, catalyzes the regio- and stereoselective hydroxylation of fatty acids. Recent work has demonstrated the importance of water in the mechanism of BM-3, and site-specific mutagenesis has helped to elucidate mechanisms of substrate recognition, binding, and product formation. One of the amino acids identified as playing a key role in the active site of BM-3 is alanine 328, which is located in the loop between the K helix and β 1−4. In the A328V BM-3 mutant, substrate affinity increases 5−10-fold and the turnover number increases 2−8-fold compared to wild-type enzyme. Unlike wild-type enzyme, this mutant is purified from *E. coli* with endogenous substrate bound due to the higher binding affinity. Close examination of the crystal structures of the substrate-bound native and A328V mutant BMPs indicates that the positioning of the substrate is essentially identical in the two forms of the enzyme, with the two valine methyl groups occupying voids present in the active site of the wild-type substrate-bound structure.

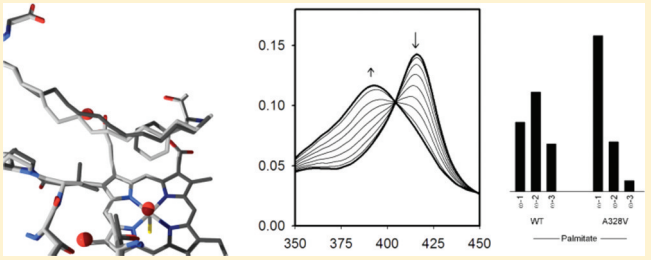

More than 65 years after the original description of pigments in microsomes isolated from liver by Albert Claude in 1943,[1] cytochrome P450 biochemistry remains a very active area of research. The enzymes are involved in a number of extremely important biochemical pathways, including but not limited to xenobiotic metabolism (including "phase I" drug metabolism), steroid hormone and bile acid biosynthesis, vitamin D metabolism, and the metabolism of numerous fatty acid derivatives involved in regulation of the kidney, heart, and vasculature.[2−6]

This superfamily of enzymes shares a common fold and a b-type heme cofactor able to complex with carbon monoxide when the heme iron is reduced to form a pigment that absorbs visible light at ∼450 nm. This absorption is unique to those hemoproteins with a cysteinyl trans-axial ligand, including the P450 and chloroperoxidase families. The absorption at 450 nm is the source of the name of this family. Most members of the family carry out monooxygenation chemistry in which molecular oxygen is reduced by NADPH-derived electrons to oxidize an organic substrate and form a molecule of water, but the enzymes carry out this chemistry on a surprisingly diverse set of organic substrates. This versatility is accomplished by combining a conserved catalytic core capable of reductively activating molecular oxygen with a variable substrate recognition region.

Most, though not all, P450 substrates are hydrophobic in nature and are made more hydrophilic by the enzymatic oxidation. In many cases the substrates also become more functionalizable, and P450-mediated oxidation is often followed by conjugation reactions like those found in "phase II" drug metabolism or in the conjugation of bile acids. The oxidation of hydrophobic substrates can often occur with strict regio- and stereospecificity, though at times it can be promiscuous. P450BM-3 has been widely studied as a model system for P450 structure and function. It oxidizes acyl chains of fatty acids and *N*-acylamino acids at the ω-1, -2, and -3 carbons with defined stereospecificity, with the binding of these hydrophobic substrates driven largely by desolvation energy.[7−9] The enzyme carries out these oxidations with incredible efficiency. This efficiency is due at least in part to the fact that rather than requiring intermolecular electron transfer to the P450 enzyme from a separate P450 reductase, P450BM-3 has a naturally self-

Received: July 15, 2011
Revised: August 26, 2011
Published: August 29, 2011

sufficient structure with both P450 reductase and P450 domains in the same polypeptide chain.[10,11]

In traditional models of catalysis, substrate binding energy must be finely balanced so that substrate binds efficiently but not too efficiently. If the substrate binds too well, the activation energy for the catalytic reaction becomes large and the reaction slows. How does this effect translate for P450s, which unlike most enzymes generate an extremely reactive enzyme-bound oxidant that will efficiently oxidize nearly any substrate held near it? In this situation, the rate of catalysis should not be significantly dependent on substrate-binding energy, unless substrate binds so tightly that product release becomes rate-limiting or the enzyme structure is destabilized. In case of P450BM-3, desolvation of the large hydrophobic surface area of substrates like palmitate and linoleic acid, along with desolvation of a hydrophobic substrate access channel in the enzyme, provides a very large driving force for substrate binding and appears to account for most of the observed substrate-binding energy.[12]

In many P450s, substrate binding is coupled to a change in the spin state of the heme iron, which has been suggested to be a potential mechanism of increasing specificity and conserving electrons.[13−19] We have shown previously that, in P450BM-3, substrate binding induces a protein conformational change that displaces the axial water ligand from the heme iron, coupling substrate binding to the change in spin state.[20−23] A small amount of substrate-binding energy is likely offset by the energy required to drive this conformational change. Because the spin-state change results in a ∼140 mV change in the reduction potential of the heme iron, it has been suggested that this change in spin-state upon substrate binding is a means to conserve electrons by keeping the heme iron in a difficult to reduce state unless a substrate molecule is present to be oxidized.[14−19]

In the course of our studies on P450BM-3, we discovered that very small changes at enzyme active site amino acid residue A328 (converting alanine to valine for example) produced dramatic changes in substrate binding, spin-state conversion, regiospecificity, and turnover rate. This observation suggested that in wild-type P450BM-3 substrate-binding energy has been finely balanced by evolution, congruent with our understanding of catalysis in general. We report here the characterization of substrate binding, spin-state conversion, catalytic activity, and protein structure in the A328V mutant relative to wild-type enzyme.

EXPERIMENTAL PROCEDURES

General Methods. The heme-binding domain of P450BM-3 and the holoenzyme were purified as previously described.[24,25] The concentrations of BMP and P450BM-3 were determined by the method of Omura and Sato.[26] UV−vis spectroscopy was performed on either a Hewlett-Packard model 8452A diode array spectrophotometer or a Varian Cary model 100 double-beam spectrophotometer. Acyl amino acid substrates were prepared as described.[8] Synthesis of the *N*-palmitoyl amino acid derivatives was reported previously.[8,27] Each of the palmitoyl amino acid derivatives was recrystallized from ethanol/10 mM HCl; purities and identities were confirmed by ^{1}H NMR and GC-MS.

Protein Expression, Purification, and Characterization. pT7BM-3 is a phagemid that expresses *cyp102* under the control of a phage T7 gene 10 promoter.[28] pT7BM-3 was a gift from Tom Poulos (University of California at Irvine). Amino acid substitution mutations were constructed using oligonucleotide-directed mutagenesis of P450BM-3 in pT7BM-3[28] using the method described by Kunkel et al.[29] Mutations were confirmed by nucleotide sequence analysis. Constructs, in the plasmid pProEx-1, contained an N-terminal hexahistidine affinity tag facilitating purification as previously reported for wild-type P450BM-3.[24,25] Constructs for mutants of the heme domain only (BMP) were created by restriction enzyme digestion of the mutated region and ligation into a similarly digested wild-type BMP construct in the plasmid vector pProEx-1. Proteins were expressed in *E. coli* DH5αF'IQ cells induced with IPTG and purified on Ni-NTA agarose followed by affinity tag removal as has been done previously for wild-type enzyme.[24,25]

The A328V mutant protein contains copurified substrate trapped in the active site (see Results section). To generate apo P450BM-3, copurified substrate was enzymatically oxidized by incubation with hexahistidine-tagged wild-type enzyme (1/2000th the amount of mutant enzyme) with 250 μM NADPH in 50 mM KPi pH 7.4. The trace amount of wild-type enzyme was then removed from the mutant protein by passing the solution over Ni-NTA. Small molecules were removed by washing the mutant protein three times using an Amicon centriprep-30 concentrator.

Spectral Titrations. For binding studies, 1.2 mL of a solution of 1 μM BMP or BMP(A328V) in 50 mM KPi, pH 7.4, were titrated with a solution of 1 mM substrate in 50 mM potassium carbonate in a stirred 1.00 cm quartz cuvette. After addition of each aliquot of substrate, the solution was allowed to equilibrate for 1 min before the UV−vis absorbance spectrum was recorded. Dissociation constants were obtained by fitting the difference between the absorbance at 418 and 394 nm to an equation describing a bimolecular association reaction.[21]

Determination of Turnover Rates and Regiospecificity of Oxidation. For measuring turnover, 50 nM P450BM-3(A328V) or wild-type P450BM-3 in 1.2 mL of 50 mM KPi pH 7.4 was equilibrated with 250 μM substrate (added from a 10 mM stock solution in 50 mM potassium carbonate). The reaction was started by the addition of NADPH to 250 μM, and the reaction was incubated at 25 °C for several minutes. The reaction was then quenched by acidification to pH 4. Reaction products were extracted by adding ethyl acetate, silylated with BSTFA/TMCS, and analyzed by GC/MS as reported previously.[8,21] Agreement between the GC/MS results and the rate of NADPH consumption (monitored by loss of UV−vis absorbance at 340 nm) was verified to ascertain that no reactions demonstrated significant uncoupling of electron consumption from organic substrate oxidation. Relative amounts of regioisomers formed were also measured similarly except that 500 μM substrate was used and the reaction was allowed to go to completion (due to the stoichiometry of this experiment, 50% of starting material would be converted to products at completion).

Complex Formation and Crystallization. For complex formation, BMP(A328V) (20 μM BMP in 50 mM KPi, pH 7.4) was titrated with 10 mM *N*-palmitoylglycine in 50 mM potassium carbonate to 10% beyond the equivalence point. The extent of complex formation was established by monitoring changes in the UV−vis spectrum. This solution was then buffer-exchanged and concentrated in an Amicon centriprep-30 concentrator to a final concentration of 84 μM (10.0 mg/

mL) in 10 mM 2-(*N*-morpholino)ethanesulfonic acid (MES), pH 6.5. The solution was stored in small aliquots at −80 °C.

Crystals of the BMP(A328V)−NPG complex were grown using vapor diffusion in the sitting drop format at 20 °C. The precipitant solution was composed of 15% (w/v) PEG-3350, 100 mM $MgCl_2$, 5% (v/v) glycerol, and 100 mM MES, pH 6.3. Equal volumes (2 μL each) of the well solution and the 10.0 mg/mL BMP−NPG complex were mixed by pipet, and the wells were sealed. After 24 h equilibration, crystallization was induced by streak seeding from lower-quality crystals grown spontaneously at higher PEG-3350 concentrations. Large numbers of crystals typically formed within 24 h. Crystals were serially transferred in steps of 5% (v/v) MPD to a final solution composed of 15% (w/v) PEG-3350, 100 mM $MgCl_2$, 5% (v/v) glycerol, 100 mM MES, pH 6.3, and 15% (v/v) MPD before being mounted in a nylon loop. Mounted crystals were flash-cooled and stored in liquid nitrogen until used for data collection.

Data Collection. Diffraction data were collected from a single crystal at 100 K, using the Advanced Photon Source 19ID beamline. BMP−NPG crystallized with the symmetry of space group $P2_1$ (unit cell constants a = 59.1 Å, b = 148.1 Å, c = 63.7 Å, b = 98.56°) and contained two molecules per asymmetric unit. All data were processed with the HKL2000 program suite.[30] Intensities were converted to structure factor amplitudes and placed on an approximate absolute scale by the program TRUNCATE in the CCP4 package.[31] Data collection and processing statistics are summarized in Table 1.

Table 1. Data Collection, Phasing, and Refinement Statistics for BMP(A328V) Structure[a]

data collection	
energy (eV)	13 119.6
resolution range (Å)	39.3−1.74 (1.80−1.74)
unique reflections	110 118 (10 856)
multiplicity	4.1 (4.0)
data completeness (%)	99.6 (98.2)
R_{merge} (%)[b]	4.5 (18.9)
$I/\sigma(I)$	27.3 (6.4)
Wilson B-value (Å^2)	20.4
refinement statistics	
resolution range (Å)	3029.6−1.74 (1.79−1.74)
no. of reflections R_{work}/R_{free}	107 915/2196 (7881/172)
data completeness (%)	99.7 (99.1)
atoms (non-H protein/heme/substrate/solvent)	7402/86/44/969
R_{work} (%)	16.5 (19.4)
R_{free} (%)	19.6 (24.2)
rmsd bond length (Å)	0.013
rmsd bond angle (deg)	1.74
mean B-value (Å^2) (protein/heme/substrate/solvent)	21.6/13.8/32.2/35.5
Ramachandran plot (%) (favored/additional/disallowed)[c]	97.7/2.3/0.0
σ_A cross-validated coordinate error (Å)	0.06
missing residues	chain A: 1, 459−470; chain B: 1, 459−470

[a]Data for the outermost shell are given in parentheses. [b]$R_{merge} = 100\sum_h\sum_i|I_{h,i} - \langle I_h\rangle|/\sum_h\sum_i I_{h,i}$, where the outer sum ($h$) is over the unique reflections and the inner sum (i) is over the set of independent observations of each unique reflection. [c]As defined by the validation suite MolProbity.[34]

Crystallographic Refinement. Refinement of the structure of BMP-NPG was carried out in the program package CNS 1.1[32] with a random 5% subset of all data set aside for R_{free} calculation. Initial model coordinates were obtained by modifying the coordinates of BMP complexed with *N*-palmitoylglycine (PDB code: 1JPZ)[21] by removing the coordinates for water molecules and the substrate. Rigid-body refinement of the model coordinates versus data between 30.0 and 1.74 Å was conducted, followed by a cycle of standard positional and group isotropic atomic displacement parameter refinement. Inspection of electron density maps in the program O[33] allowed a model for the substrate to be added. Subsequent cycles of standard positional and individual isotropic atomic displacement parameter refinement coupled with cycles of model rebuilding, modeling of alternate conformations, and addition of solvent molecules were carried out against all data from 30.0 to 1.74 Å. Complete refinement statistics for the structure are listed in Table 1.

RESULTS

Mutagenesis, Protein Purification, and Initial Characterization. In the course of modeling studies to identify active-site residues of P450BM-3 that determine substrate specificity, we predicted that alteration of residue A328 would alter substrate specificity, as the methyl side chain is located immediately adjacent to the heme iron on the distal side of the heme. A pair of mutants of P450BM-3, A328V and A328S, was generated. Initial characterization with substrates revealed unusual spin-state behavior upon substrate binding. To characterize the cause of the altered behavior, both mutant holoenzymes (P450BM-3) and isolated heme domains (BMP) were subcloned, expressed, and purified. The characterization of the A328V mutant is reported here.

Initial spectra of the BMP(A328V) mutant revealed that the enzyme was isolated predominantly in the high-spin state as indicated by a Soret band maximum in the UV−vis spectrum at 392 nm. Extensive dilution of the enzyme resulted in spectral changes consistent with the conversion of a small amount of high-spin BMP(A328V) to the low-spin state, suggesting that the protein had been purified with substrate bound in the active site and slight dissociation occurred upon dilution. To deplete any P450BM-3 substrate associated with the high-spin BMP(A328V), the protein was incubated with a small amount of highly active wild-type P450BM-3 at a molar ratio of 2000:1 with 250 μM NADPH, resulting in a rapid conversion of the BMP(A328V) from almost completely high spin to low spin as the substrate was oxidized by the wild-type enzyme. The mutant protein was then repurified from this mixture by a second Ni-NTA column. It should be noted that even after this last purification the A328V constructs had a tendency to return to the high-spin state when exposed to plastic, presumably due to the binding of hydrophobic compounds present in many plastics (for example, oleamide and benzalkonium chlorides, although the compounds bound to the enzyme were not identified).[35] Great care had to be taken to prevent contamination of the enzyme samples.

Spectral Characterization. Once treated as described above, the A328V mutant enzymes were observed to exist in a low-spin state. As can be seen in Figure 1 (which shows spectra for only the BMP constructs, P450BM-3 constructs were comparable), the mutant enzyme has a Soret band maximum near 420 nm similar to wild-type enzyme. Titration of the mutants with the high-affinity P450BM-3 substrate *N*-

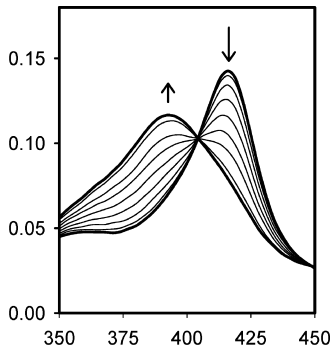

Figure 1. Titration of BMP(A328V) with palmitate. BMP(A328V), 1 μM, in 50 mM KPi, pH 7. Four was titrated with sequential aliquots of 25 mM palmitic acid in 50 mM K_2CO_3. Maximal absorbance in the absence of substrate is at 418 nm. Upon saturation with substrate the absorbance maximum is shifted to 392 nm.

palmitoylglycine resulted in the efficient conversion of BMP(A328V) to a high-spin form (the peak at 420 nm largely disappears and a new peak at 392 nm appears) similar to the changes observed in the wild-type enzyme.

Substrate Binding. More detailed analysis of the affinities of various substrates for the mutants using similar titrations appears in Table 2. All substrates gave efficient conversion of

Table 2. Substrate Dissociation Constants Determined by UV−vis Titration[b]

substrate[a]	BMP(wt) dissociation const (nM)[b]	BMP(A328V) dissociation const (nM)[b]	fold enhancement
palmitate	1300 ± 170	160 ± 20	8.1
PalmGly	320 ± 10	45 ± 14	7.1
PalmMet	<30[c]	<30[c]	ND[d]
PalmLeu	<30[c]	<30[c]	ND[d]
PalmGln	200 ± 14	74 ± 5	2.7
PalmGlu	3700 ± 130	410 ± 60	9.0

[a]*N*-Palmitoylated L-amino acids are listed by the abbreviation Palm*Xxx*, where *Xxx* is the three letter code for the appropriate amino acid. [b]Titrations were carried out in 50 mM KPi pH 7.4 at room temperature with 1 μM P450 and the variation in absorbance (the difference between the absorbance at 418 and 392 nm) as a function of substrate concentration was fit to an equation for bimolecular association to determine the dissociation equilibrium constant K_D (data were corrected for enzyme dilution that in no case was more than 5% over the course of the titration). [c]Because of the constraints of the UV−vis binding assay, dissociation constants of less than 30 nM demonstrate essentially stoichiometric binding and the true K_D cannot be determined. [d]ND = not determined due to the uncertainty in the individual K_Ds.

the enzyme from the low-spin state to the high-spin state upon saturation with substrate. The substrate affinity of the A328V mutant is at least 2.7 times that of the wild-type enzyme and in some cases increases up to 9-fold (two compounds bound too tightly to accurately measure the dissociation constant with this assay). The greatest increase in affinity occurred for the weakest binding substrates.

Catalysis. In order to determine whether the variation in substrate affinity affected the rate of catalysis, initial-rate kinetics at high (250 μM) concentrations of substrate were carried out with P450BM-3 and P450BM-3(A328V). As can be shown in Table 3, the A328V mutant carried out oxidation at

Table 3. Mutations Affect Turnover

substrate	BM-3(wt)[a]	BM-3(A328V)[a]	fold enhancement[b]
palmitate	1480 ± 35	3355 ± 95	2.3
PalmGly	1875 ± 30	5500 ± 600	2.9
PalmMet	1690 ± 75	4400 ± 145	2.6
PalmLeu	1155 ± 20	3900 ± 320	3.4
PalmGln	610 ± 25	4500 ± 500	7.4
PalmGlu	485 ± 15	3960 ± 280	8.2
geranyl acetone[c]	324 ± 17	550 ± 72	2.2
neryl acetone[c]	155 ± 7	338 ± 10	1.7

[a]Steady-state kinetics were measured with 50 nM enzyme and 250 μM substrate in 50 mM KPi buffer pH 7.4 at 25 °C. Products were quantified by GC-MS. Results are displayed as turnover rates in μmol/min/μmol. [b]Fold enhancement is the rate for the A328V mutant divided by the rate for wild-type enzyme. [c]From ref 36, under similar conditions but determined with 2% (v/v) DMSO, 200 μM substrate, and 500 nM enzyme.

least twice the rate of wild-type enzyme for every substrate tested and in some cases demonstrated 8-fold faster turnover. Rates increased the most for the substrates with lower rates of reaction for wild-type enzyme, and the entire set of substrates gave similarly high rates with the A328V mutant. Note that for all substrates the concentration of 250 μM is expected to be saturating, as the highest dissociation constant for wild-type enzyme was 3.7 μM and for the A328V mutant was 0.41 μM. It was suggested that the first electron transfer to the heme domain is the rate-limiting step in P450BM-3 catalysis, and the high rates of turnover in the A328V mutant approach the maximal rates of electron transfer through the flavoprotein domains of the enzyme as measured by cytochrome *c* reduction kinetics.[11] These rates were determined by GC/MS analysis of the oxidized organic products, not by NADPH consumption, so the high rates of reaction cannot be explained by uncoupling of electron transfer from substrate oxidation in the mutant enzymes. An increase in rate for the A328V mutation has also been noted in screens for oxidation of geranyl acetone and neryl acetone by rationally designed mutant libraries, with 1.7−2.2-fold enhancement over wild-type oxidation rates.[36]

Wild-type P450BM-3 catalyzes the oxidation of palmitate and palmitoylated-amino acid derivatives predominantly at the ω-1, ω-2, and ω-3 carbons of the fatty acyl chains. In order to examine the regiospecificity of hydroxylation in the mutant, both palmitate and myristate were incubated with P450BM-3 and P450BM-3(A328V) and the distribution of products analyzed by GC/MS (Figure 2). Compared to wild-type enzyme, the A328V mutant demonstrates a dramatically different product distribution, which heavily favors oxidation at the ω-1 position and shows almost no oxidation at the ω-3 position. In the case of palmitate, wild-type enzyme produces ω-2 hydroxypalmitate as the major product (46% of total products), whereas the ω-1 hydroxypalmitate is the major product (72%) for the A328V mutant. This observation clearly suggests that the conformation of the substrate acyl chain is different in the mutant and wild-type enzymes, at least at the time of hydrogen atom abstraction. As will be discussed later, the conformation of substrate in the resting, oxidized form and in the reduced form of the wild-type enzyme have been shown to be different, although the conformation in the reduced form of the enzyme is not known.[37]

Structure Determination. Because the data on rate of reaction, substrate affinity, and oxidation regiospecificity

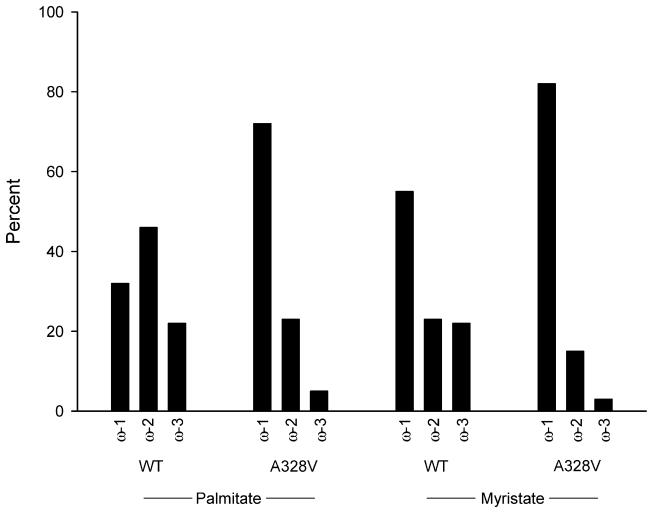

Figure 2. P450BM-3 hydroxylates fatty-acid substrates at the ω-1, ω-2, and ω-3 positions. Relative amounts of each product were determined by the area of the appropriate peak from GC-MS of BSTFA/TMCS derivatives, which give similar response factors for each regioisomer. Product mixtures were prepared by incubating 500 μM substrate with 50 nM P450BM-3 or P450BM-3(A328V) in 50 mM KPi, pH 7.4. NADPH was added to 250 μM, the reaction allowed to run to completion, and the products were derivatized and analyzed. Results are expressed as percent of total oxidation products.

demonstrated clear differences in substrate binding between mutant and wild-type enzymes, we attempted to crystallize the mutant in both substrate-free and *N*-palmitoylglycine-bound forms so that the protein structure and substrate conformation could be compared to that of wild-type enzyme. We were able to obtain crystals of the BMP(A328V) construct only in the substrate-bound form. When the initially substrate-free form of BMP(A328V) was crystallized, the crystalline protein was always found to be in the substrate-bound form. Spectroscopic studies had suggested that this mutant enzyme has an extremely high propensity to bind to hydrophobic molecules from its environment as mentioned previously. We did not characterize the structure of these crystals with unknown environmental ligands bound, but rather focused on crystals of the *N*-palmitoylglcyine-bound enzyme. The crystals of BMP(A328V) with *N*-palmitoylglycine bound isomorphous to the wild-type BMP−substrate complex (PDB 1JPZ).[21] Crystals of substrate-bound BMP(A328V) diffracted to a Bragg spacing (d_{min}) of 1.74 Å. The final model contains residues 2−458 for chains A and B, two hemes, two *N*-palmitoylglycines, one MES molecule, one glycerol molecule, and 933 water molecules (final R = 16.5; R_{free} = 19.6). Data collection and refinement statistics are shown in Table 1.

The crystal structures revealed strikingly little deviation between the structure of the protein and position of the substrate between the mutant and wild type (Figure 3). In both structures, the F- and G-helices and the loop connecting them have moved toward the substrate, closing off the substrate access channel. The conformations of these helices and the backbone of the proteins in general are essentially identical between the wild type and the A328V mutant.

Substrate binds to the wild-type and mutant enzymes in a similar conformation. The substrates for P450BM-3 are fatty acids and *N*-acylamino acids, both of which consist of a long hydrophobic acyl chain and a polar headgroup that interacts with the enzyme via multiple hydrogen bonds and electrostatic interactions. The polar carboxylate group of fatty acids was first shown to interact with Y51 via hydrogen bonding and R47 via electrostatic interactions in crystal structures of the BMP−palmitoleic acid complex.[23] We later established that the amide carbonyl of *N*-acylamino acids also hydrogen bonds with Y51, although the amino acid carboxylate interacts with the free N-terminus of the B′-helix.[8,21] In both cases substrates are "anchored" at this position via the polar interactions. In the A328V−palmitoylglycine complex, these interactions are all essentially identical to those observed with wild-type enzyme.

Near the omega end of the fatty acyl chain, where oxidation occurs, subtle differences could be observed in the exact position of the substrate within the active site. A direct comparison of wild-type enzyme and A328V complexed with *N*-palmitoylglycine is shown in Figure 4. The primary effect of the mutation on the positioning of the substrate is observed where the substrate immediately contacts the mutated amino acid side chain. At this point the substrate appears to move slightly away from A328 to accommodate the new valine methyl group. In fact, other than this slight perturbation of substrate, very little difference between the active site structures in wild-type and A328V enzyme can be detected. The one other noticeable change is an extremely small perturbation in the side chain of T268, the highly conserved threonine believed to be important in the delivery of protons and scission of dioxygen carried out by the enzyme. Like the substrate acyl chain, the T268 side chain moves slightly away from A328 to accommodate the additional new methyl group. Close examination of the structure (not shown) reveals that small perturbations are required in the A328V structure in order to alleviate a direct steric conflict between the A328V side chain and both the T268 methyl group and substrate acyl chain (in their positions in the wild-type enzyme−substrate complex). Beyond these steric conflicts, the methyl groups are very well tolerated at least in part due to the fact that there exist voids or water molecules around the side chain of residue A328 in wild-type enzyme. Thus, the effective addition of two methyl groups by the alanine to valine mutation is well tolerated by the protein structure.

DISCUSSION

What causes the striking differences in behavior between the wild-type and mutant enzymes, when there is so little difference in their structures? First, a straightforward explanation arises for the increased affinity of substrates for the A328V mutant relative to wild-type enzyme when one examines models of amino acid hydrophobicity. The difference in the free energy of desolvation of the side chains of alanine and valine from three relevant models[39−42] is 3.9 ± 0.2 kJ/mol. This difference provides a good estimate of the amount of binding energy gained by the mutation in the absence of detrimental steric conflicts between the protein and substrate, and the presence of structurally conserved active-site water molecules in the wild-type versus mutant structures. The average gain in binding energy from the wild type to A328V mutant for the four substrates with dissociation constants determined for both proteins (palmitate, PalmGly, PalmGlu, and PalmGln) is 4.7 ± 0.9 kJ/mol. Clearly, the 3.9 kJ/mol predicted by the difference in desolvation of the amino acid side chain agrees well with this average, and protein desolvation likely accounts for a majority of the gain in substrate affinity.

How can the high rate of turnover in the A328V P450BM-3 mutant be explained? In addition to the normal interplay of

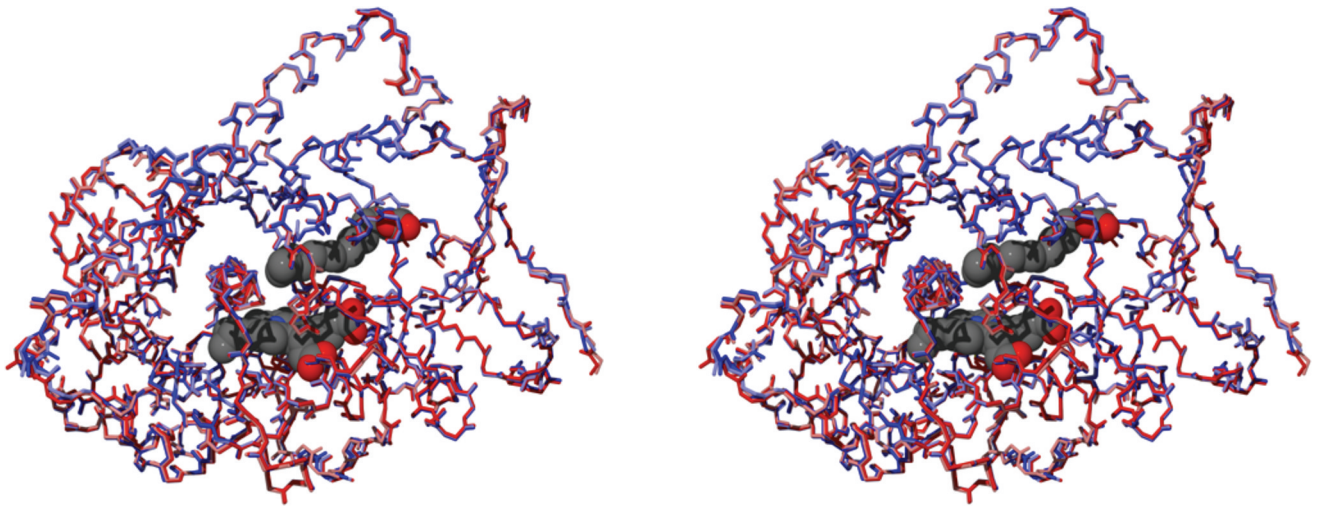

Figure 3. Stereo backbone alignment of BMP and BMP(A328V). Molecule A from the wild-type structure 1JPZ (light red), molecule B from 1JPZ (dark red), molecule A from the A328V mutant structure 1ZOA (dark blue), and molecule B from the A328V mutant structure (light blue) were aligned, and backbone atoms are shown along with the heme (center) and *N*-palmitoylglycine molecules (just above and to the right of heme). For clarity, the heme and substrate are only shown for the last of these structures. This figure was created using Swiss PDB-Viewer in conjunction with POV-Ray.[38]

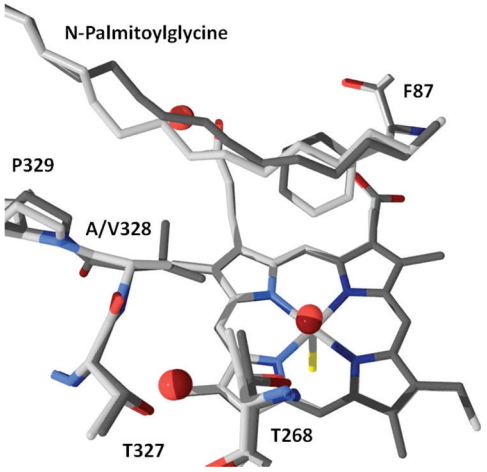

Figure 4. Comparison of acyl-chain positioning in the active site of substrate-bound wild-type BMP (light colors, from PDB 1JPZ molecule A) and BMP(A328V) (dark, PDB 1ZOA molecule A). Crystallographically ordered water molecules are represented as red spheres.

substrate-binding energy and catalysis observed in enzymes, upon binding substrate P450BM-3 undergoes a change in the spin state of the heme iron that can directly impact the reaction rate via a redox potential change. This spin-state change is known to make reduction of the heme more favorable, as the redox potential shifts by ~140 mV.[43−46] It has been proposed that this change in redox potential represents a gating mechanism in P450s in general, helping to keep electrons from being wasted by transfer to P450s that lack substrates to be oxidized and that transfer of the first electron is the rate-limiting step in P450BM-3.[47] Since both wild type and A328V P450BM-3 efficiently change from the low-spin to the high-spin state upon substrate binding, differences in the resulting turnover rate deriving from spin-state-driven redox-potential changes would be expected to be relatively small. The A328V mutation resulted in unexpectedly high turnover rates, however. Since the rates shown in Table 3 were measured by direct GC/MS quantification of oxidized products, they are not an artifact of uncoupling of electron transport from substrate oxidation (a common problem when rates are measured by monitoring consumption of NADPH by UV−vis).

Our recent estimates of the rate of electron transfer through the FAD and FMN domains of the dimeric enzyme using cytochrome *c* reduction kinetics (cytochrome *c* is reduced by the FMN domain just as BMP is when substrate is bound) at high enzyme concentrations established the maximal rate of reduction under very similar conditions to those used in the current study as 5390 ± 170 μmol/(min μmol) for wild-type P450BM-3.[11] Because this rate is a measure of electron transfer through the reductase domains of the enzymes, it is unlikely that a mutation in the buried active site of the heme domain would perturb it significantly. When compared to the maximal rate of substrate oxidation reported here of 5500 ± 600 μmol/(min μmol), transfer of the first electron would certainly appear to be strongly rate-limiting in the A328V mutant with the best substrates. It would appear that in wild-type enzyme transfer of the first electron is only partially rate-limiting, but in the A328V mutant it becomes the major limiting step. Thus, by extension of this logic, the effect of the A328V mutant appears to be to speed up a step in the mechanism of P450BM-3 (other than transfer of the first electron to the heme domain) that is partially rate-limiting in wild-type enzyme. This step is no longer partially limiting the rate in the A328V mutant, leaving the transfer of the first electron as the major rate-determining factor. It should be noted that the transfer of the second electron has been suggested to be rate-limiting in some mutants of P450BM-3.[48] The transfer of the second electron is certainly a good candidate for the step that may be sped up by A328V mutation in our study.

The regiospecificity difference between the mutant and wild-type enzyme does not appear to stem from the conformation of the resting, oxidized enzyme/substrate complex because the carbon atoms in question occupy essentially identical positions in the crystal structures of the enzymes. Although it is possible that these crystal structures do not represent the true resting conformation of the substrate at room temperature, and some

dx.doi.org/10.1021/bi201099j | *Biochemistry* 2011, 50, 8333−8341

have suggested that local changes in active-site structure may occur upon lowering the temperature of the enzyme; e.g., during X-ray diffraction data collection,[49−53] it seems likely that the major differences observed stem from the conformation of the substrate in the active site after the enzyme is reduced by the transfer of the first electron, normally the rate-limiting step for P450BM-3. Until hydrogen atom abstraction, any of the observed regioisomers may still be formed so certainly the differing regiospecificity of wild-type and A328S enzymes involves a difference in conformation at that step, which occurs later in the mechanism than transfer of the first electron. NMR studies have shown that at room temperature a change in substrate position occurs upon the first reduction of the enzyme,[37] which is also suggested by the excessive distance of the oxidized carbon atoms from the heme iron in the resting structures,[8,21,23] although the exact nature of this conformational change has never been determined.

Our data clearly show that the A328V mutant of P450BM-3 can bind substrates more tightly and catalyze their oxidation more efficiently than the wild-type enzyme. P450BM-3 belongs to a family of cytochrome P450 enzymes known as the CYP102 family, members of which share at least 40% amino acid sequence identity. An examination of all CYP102 family members listed in David Nelson's Cytochrome P450 Homepage (http://drnelson.uthsc.edu/blast/allbacteria.htm)[54] reveals that 25 of 26 sequences available have Ala at this position, and one has Ile (CYP102D1 has Ile but also has a disruption of nearby pralines in this region of the sequence). Why does nearly every member of the CYP102 family sequenced to date have the conserved alanine at this position, suggesting there is strong selection pressure at this site to maintain sequence conservation even though the enzyme is more active with valine at this position? Perhaps in the complicated milieu of the host cell the residue helps exclude substrates whose oxidation is detrimental to the cell. It may be that the altered regiospecificity is problematic, as the A328V mutant forms almost entirely ω-1 hydroxylated product, but it is unknown if this is the most physiologically important oxidation product. The true physiological substrate for the reaction may not be a fatty acid or acyl amino acid, even though oxidation of these compounds by P450BM-3 has now been studied for almost 30 years, but some other hydrophobic compound that may fit in the active site differently and require the more open active site of the native enzyme.

P450BM-3 has been extensively used in recent years as a template to generate novel catalysts using library-generation and screening techniques. It is interesting to note that although nature has not made use of the A328V mutation, it has been identified as one of the mutations that occurs in several positive "hits" from screens of mutant libraries developed to make an enzyme that is capable of oxidizing non-native substrates.[36,55−58] In fact, in at least one of the studies the rate of substrate oxidation by P450BM-3 A328V and the respective wild-type activity can be directly compared and a similar ∼2-fold rate increase in rate upon introduction of the mutation was observed.[36] The data and analysis reported here reveal that the A328V mutant is also beneficial for fatty acid and acyl amino acid oxidation and suggest that the benefit stems from two different mechanisms: (1) increased affinity for hydrophobic substrates enhancing the formation of the enzyme−substrate complex and (2) enhanced rate of catalysis once substrate is bound, most likely due to currently unknown alterations in the active-site conformation during steps in the P450BM-3 mechanism that occur after the first electron reduction.

■ ASSOCIATED CONTENT

Accession Codes

The coordinates and structure factors for the A328V mutant have been deposited with the Protein Data Bank and assigned the identification code 1ZOA.

■ AUTHOR INFORMATION

Corresponding Author

*Ph: 936-294-1530. Fax: 936-294-4996. E-mail: Haines@SHSU.edu.

Funding

This research was supported in part by research grants GM43479 and GM50858 from the NIH (J.A.P.) and X-011 from the Robert A. Welch Foundation (D.C.H.).

■ ACKNOWLEDGMENTS

Results shown in this report are derived from work performed at Argonne National Laboratory, Structural Biology Center at the Advanced Photon Source. Argonne is operated by UChicago Argonne, LLC, for the U.S. Department of Energy, Office of Biological and Environmental Research, under Contract DE-AC02-06CH11357.

■ ABBREVIATIONS

BMP, the heme domain of P450 BM-3; BM-3, P450BM-3; IPTG, isopropyl-β-D-thiogalactoside; Ni-NTA, nickel-nitrilotriacetic acid; KPi, potassium phosphate; BSTFA/TMCS, *N*,*O*-bis(trimethylsilyl)trifluoroacetamide with 1% trimethylchlorosilane; GC/MS, gas chromatograph/mass spectrometer; MES, 2-(*N*-morpholino)ethanesulfonic acid; MPD, 2-methyl-2,4-pentanediol; PalmGly, *N*-palmitoylglycine; PalmGlu, *N*-palmitoyl-L-glutamate; PalmGln, *N*-palmitoyl-L-glutamine; PalmMet, *N*-palmitoyl-L-methionine.

■ REFERENCES

(1) Claude, A. (1943) The Constitution of Protoplasm. *Science 97*, 451−456.

(2) Capdevila, J. H., Harris, R. C., and Falck, J. R. (2002) Microsomal cytochrome P450 and eicosanoid metabolism. *Cell. Mol. Life Sci. 59*, 780−789.

(3) Anzenbacher, P., and Anzenbacherova, E. (2001) Cytochromes P450 and metabolism of xenobiotics. *Cell. Mol. Life Sci. 58*, 737−747.

(4) Lewis, D. F. (1996) *Cytochromes P450: Structure, Function, and Mechanism*, Vol. *1*, Taylor & Francis, London.

(5) Pikuleva, I. A. (2006) Cytochrome P450s and cholesterol homeostasis. *Pharmacol. Ther. 112*, 761−773.

(6) Werck-Reichhart, D., and Feyereisen, R. (2000) Cytochromes P450: a success story, *Genome Biol. 1*, REVIEWS3003.

(7) Chowdhary, P. K., Keshavan, N., Nguyen, H. Q., Peterson, J. A., Gonzalez, J. E., and Haines, D. C. (2007) Bacillus megaterium CYP102A1 Oxidation of Acyl Homoserine Lactones and Acyl Homoserines. *Biochemistry 46*, 14429−14437.

(8) Hegde, A., Haines, D. C., Bondlela, M., Chen, B., Schaffer, N., Tomchick, D. R., Machius, M., Nguyen, H., Chowdhary, P. K., Stewart, L., Lopez, C., and Peterson, J. A. (2007) Interactions of substrates at the surface of p450s can greatly enhance substrate potency. *Biochemistry 46*, 14010−14017.

(9) Haines, D. C., Chen, B., Tomchick, D. R., Bondlela, M., Hegde, A., Machius, M., and Peterson, J. A. (2008) Crystal structure of inhibitor-bound P450BM-3 reveals open conformation of substrate access channel. *Biochemistry 47*, 3662−3670.

(10) Haines, D. C., Sevrioukova, I. F., and Peterson, J. A. (2000) The FMN-binding domain of cytochrome P450BM-3: resolution, reconstitution, and flavin analogue substitution. *Biochemistry 39*, 9419−9429.
(11) Kitazume, T., Haines, D. C., Estabrook, R. W., Chen, B., and Peterson, J. A. (2007) Obligatory intermolecular electron-transfer from FAD to FMN in dimeric P450BM-3. *Biochemistry 46*, 11892−11901.
(12) Lewis, D. F., Eddershaw, P. J., Dickins, M., Tarbit, M. H., and Goldfarb, P. S. (1998) Structural determinants of cytochrome P450 substrate specificity, binding affinity and catalytic rate. *Chem. Biol. Interact. 115*, 175−199.
(13) Hasemann, C. A., Kurumbail, R. G., Boddupalli, S. S., Peterson, J. A., and Deisenhofer, J. (1995) Structure and function of cytochromes P450: a comparative analysis of three crystal structures. *Structure 3*, 41−62.
(14) Backes, W. L., Tamburini, P. P., Jansson, I., Gibson, G. G., Sligar, S. G., and Schenkman, J. B. (1985) Kinetics of cytochrome P-450 reduction: evidence for faster reduction of the high-spin ferric state. *Biochemistry 24*, 5130−5136.
(15) Tamburini, P. P., Gibson, G. G., Backes, W. L., Sligar, S. G., and Schenkman, J. B. (1984) Reduction kinetics of purified rat liver cytochrome P-450. Evidence for a sequential reaction mechanism dependent on the hemoprotein spin state. *Biochemistry 23*, 4526−4533.
(16) Backes, W. L., Sligar, S. G., and Schenkman, J. B. (1982) Kinetics of hepatic cytochrome P-450 reduction: correlation with spin state of the ferric heme. *Biochemistry 21*, 1324−1330.
(17) Gibson, G. G., Sligar, S. G., Cinti, D. L., and Schenkman, J. B. (1980) Purified cytochrome P-450: spin-state control of the haemoprotein redox potential [proceedings]. *Biochem. Soc. Trans. 8*, 101−102.
(18) Sligar, S. G., Cinti, D. L., Gibson, G. G., and Schenkman, J. B. (1979) Spin state control of the hepatic cytochrome P450 redox potential. *Biochem. Biophys. Res. Commun. 90*, 925−932.
(19) Sligar, S. G. (1976) Coupling of spin, substrate, and redox equilibria in cytochrome P450. *Biochemistry 15*, 5399−5406.
(20) Narhi, L. O., and Fulco, A. J. (1987) Identification and characterization of two functional domains in cytochrome P-450BM-3, a catalytically self-sufficient monooxygenase induced by barbiturates in Bacillus megaterium. *J. Biol. Chem. 262*, 6683−6690.
(21) Haines, D. C., Tomchick, D. R., Machius, M., and Peterson, J. A. (2001) Pivotal role of water in the mechanism of P450BM-3. *Biochemistry 40*, 13456−13465.
(22) Deng, T. J., Proniewicz, L. M., Kincaid, J. R., Yeom, H., Macdonald, I. D., and Sligar, S. G. (1999) Resonance Raman studies of cytochrome P450BM3 and its complexes with exogenous ligands. *Biochemistry 38*, 13699−13706.
(23) Li, H., and Poulos, T. L. (1997) The structure of the cytochrome p450BM-3 haem domain complexed with the fatty acid substrate, palmitoleic acid. *Nat. Struct. Biol. 4*, 140−146.
(24) Sevrioukova, I., Truan, G., and Peterson, J. A. (1996) The flavoprotein domain of P450BM-3: expression, purification, and properties of the flavin adenine dinucleotide- and flavin mononucleotide-binding subdomains. *Biochemistry 35*, 7528−7535.
(25) Boddupalli, S. S., Hasemann, C. A., Ravichandran, K. G., Lu, J. Y., Goldsmith, E. J., Deisenhofer, J., and Peterson, J. A. (1992) Crystallization and preliminary x-ray diffraction analysis of P450terp and the hemoprotein domain of P450BM-3, enzymes belonging to two distinct classes of the cytochrome P450 superfamily. *Proc. Natl. Acad. Sci. U. S. A. 89*, 5567−5571.
(26) Omura, T., and Sato, R. (1964) The Carbon Monoxide-Binding Pigment of Liver Microsomes. I. Evidence for Its Hemoprotein Nature. *J. Biol. Chem. 239*, 2370−2378.
(27) Lapidot, Y., Rappoport, S., and Wolman, Y. (1967) Use of esters of N-hydroxysuccinimide in the synthesis of N-acylamino acids. *J. Lipid Res. 8*, 142−145.
(28) Darwish, K., Li, H. Y., and Poulos, T. L. (1991) Engineering proteins, subcloning and hyperexpressing oxidoreductase genes. *Protein Eng. 4*, 701−708.
(29) Kunkel, T. A., Roberts, J. D., and Zakour, R. A. (1987) Rapid and efficient site-specific mutagenesis without phenotypic selection. *Methods Enzymol. 154*, 367−382.
(30) Otwinowski, Z., and Minor, W. (1997) Processing of X-ray diffraction data collected in oscillation mode. *Methods Enzymol. 276*, 307−326.
(31) French, S., and Wilson, K. (1978) On the treatment of negative intensity observations. *Acta Crystallogr., Sect. A: Found. Crystallogr. 34*, 517−525.
(32) Brunger, A. T., Adams, P. D., Clore, G. M., DeLano, W. L., Gros, P., Grosse-Kunstleve, R. W., Jiang, J. S., Kuszewski, J., Nilges, M., Pannu, N. S., Read, R. J., Rice, L. M., Simonson, T., and Warren, G. L. (1998) Crystallography & NMR system: A new software suite for macromolecular structure determination. *Acta Crystallogr., Sect. D: Biol. Crystallogr. 54* (Pt5), 905−921.
(33) Jones, T. A., Zou, J. Y., Cowan, S. W., and Kjeldgaard. (1991) Improved methods for building protein models in electron density maps and the location of errors in these models. *Acta Crystallogr., Sect. D: Biol. Crystallogr. 47* (Pt 2), 110−119.
(34) Davis, I. W., Leaver-Fay, A., Chen, V. B., Block, J. N., Kapral, G. J., Wang, X., Murray, L. W., Arendall, W. B. III, Snoeyink, J., Richardson, J. S., and Richardson, D. C. (2007) MolProbity: all-atom contacts and structure validation for proteins and nucleic acids. *Nucleic Acids Res. 35*, W375−383.
(35) McDonald, G. R., Hudson, A. L., Dunn, S. M., You, H., Baker, G. B., Whittal, R. M., Martin, J. W., Jha, A., Edmondson, D. E., and Holt, A. (2008) Bioactive contaminants leach from disposable laboratory plasticware. *Science 322*, 917.
(36) Seifert, A., Vomund, S., Grohmann, K., Kriening, S., Urlacher, V. B., Laschat, S., and Pleiss, J. (2009) Rational design of a minimal and highly enriched CYP102A1 mutant library with improved regio-, stereo- and chemoselectivity. *ChemBioChem 10*, 853−861.
(37) Modi, S., Sutcliffe, M. J., Primrose, W. U., Lian, L. Y., and Roberts, G. C. (1996) The catalytic mechanism of cytochrome P450 BM3 involves a 6 A movement of the bound substrate on reduction. *Nat. Struct. Biol. 3*, 414−417.
(38) Guex, N., and Peitsch, M. C. (1997) SWISS-MODEL and the Swiss-PdbViewer: an environment for comparative protein modeling. *Electrophoresis 18*, 2714−2723.
(39) Creighton, T. E. (1993) *Proteins: Structures and Molecular Properties*, 2nd ed., W.H. Freeman, New York.
(40) Levitt, M. (1976) A simplified representation of protein conformations for rapid simulation of protein folding. *J. Mol. Biol. 104*, 59−107.
(41) Nozaki, Y., and Tanford, C. (1971) The solubility of amino acids and two glycine peptides in aqueous ethanol and dioxane solutions. Establishment of a hydrophobicity scale. *J. Biol. Chem. 246*, 2211−2217.
(42) Roseman, M. A. (1988) Hydrophilicity of polar amino acid side-chains is markedly reduced by flanking peptide bonds. *J. Mol. Biol. 200*, 513−522.
(43) Clark, J. P., Miles, C. S., Mowat, C. G., Walkinshaw, M. D., Reid, G. A., Daff, S. N., and Chapman, S. K. (2006) The role of Thr268 and Phe393 in cytochrome P450 BM3. *J. Inorg. Biochem. 100*, 1075−1090.
(44) Ost, T. W., Miles, C. S., Munro, A. W., Murdoch, J., Reid, G. A., and Chapman, S. K. (2001) Phenylalanine 393 exerts thermodynamic control over the heme of flavocytochrome P450 BM3. *Biochemistry 40*, 13421−13429.
(45) Ost, T. W., Munro, A. W., Mowat, C. G., Taylor, P. R., Pesseguiero, A., Fulco, A. J., Cho, A. K., Cheesman, M. A., Walkinshaw, M. D., and Chapman, S. K. (2001) Structural and spectroscopic analysis of the F393H mutant of flavocytochrome P450 BM3. *Biochemistry 40*, 13430−13438.
(46) Chen, Z., Ost, T. W., and Schelvis, J. P. (2004) Phe393 mutants of cytochrome P450 BM3 with modified heme redox potentials have altered heme vinyl and propionate conformations. *Biochemistry 43*, 1798−1808.
(47) Noble, M. A., Miles, C. S., Chapman, S. K., Lysek, D. A., MacKay, A. C., Reid, G. A., Hanzlik, R. P., and Munro, A. W. (1999)

Roles of key active-site residues in flavocytochrome P450 BM3. *Biochem. J. 339* (Pt 2), 371−379.
(48) Ost, T. W., Clark, J., Mowat, C. G., Miles, C. S., Walkinshaw, M. D., Reid, G. A., Chapman, S. K., and Daff, S. (2003) Oxygen activation and electron transfer in flavocytochrome P450 BM3. *J. Am. Chem. Soc. 125*, 15010−15020.
(49) Brenner, S., Hay, S., Girvan, H. M., Munro, A. W., and Scrutton, N. S. (2007) Conformational dynamics of the cytochrome P450 BM3/N-palmitoylglycine complex: the proposed "proximal-distal" transition probed by temperature-jump spectroscopy. *J. Phys. Chem. B 111*, 7879−7886.
(50) Ravindranathan, K. P., Gallicchio, E., McDermott, A. E., and Levy, R. M. (2007) Conformational dynamics of substrate in the active site of cytochrome P450 BM-3/NPG complex: insights from NMR order parameters. *J. Am. Chem. Soc. 129*, 474−475.
(51) Ravindranathan, K. P., Gallicchio, E., Friesner, R. A., McDermott, A. E., and Levy, R. M. (2006) Conformational equilibrium of cytochrome P450 BM-3 complexed with N-palmitoylglycine: a replica exchange molecular dynamics study. *J. Am. Chem. Soc. 128*, 5786−5791.
(52) Jovanovic, T., and McDermott, A. E. (2005) Observation of ligand binding to cytochrome P450 BM-3 by means of solid-state NMR spectroscopy. *J. Am. Chem. Soc. 127*, 13816−13821.
(53) Jovanovic, T., Farid, R., Friesner, R. A., and McDermott, A. E. (2005) Thermal equilibrium of high- and low-spin forms of cytochrome P450 BM-3: repositioning of the substrate? *J. Am. Chem. Soc. 127*, 13548−13552.
(54) Nelson, D. R. (2009) The cytochrome p450 homepage. *Hum. Genomics 4*, 59−65.
(55) Peters, M. W., Meinhold, P., Glieder, A., and Arnold, F. H. (2003) Regio- and enantioselective alkane hydroxylation with engineered cytochromes P450 BM-3. *J. Am. Chem. Soc. 125*, 13442−13450.
(56) Kubo, T., Peters, M. W., Meinhold, P., and Arnold, F. H. (2006) Enantioselective epoxidation of terminal alkenes to (R)- and (S)-epoxides by engineered cytochromes P450 BM-3. *Chemistry 12*, 1216−1220.
(57) Munzer, D. F., Meinhold, P., Peters, M. W., Feichtenhofer, S., Griengl, H., Arnold, F. H., Glieder, A., and de Raadt, A. (2005) Stereoselective hydroxylation of an achiral cyclopentanecarboxylic acid derivative using engineered P450s BM-3. *Chem. Commun. (Cambridge, U. K.)*, 2597−2599.
(58) Weber, E., Seifert, A., Antonovici, M., Geinitz, C., Pleiss, J., and Urlacher, V. B. (2011) Screening of a minimal enriched P450 BM3 mutant library for hydroxylation of cyclic and acyclic alkanes. *Chem. Commun. (Cambridge, U. K.) 47*, 944−946.